Facile fabrication of microperforated membranes with re-useable SU-8 molds for organs-on-chips

de Haan, Pim; Mathwig, Klaus; Yuan, Lu; Peterson, Brandon W.; Verpoorte, Elisabeth

Published in:
Organs-on-a-Chip

DOI:
10.1016/j.ooc.2023.100026

Publication date:
2023

Organs-on-a-Chip 5 (2023) 100026

Contents lists available at ScienceDirect

Organs-on-a-Chip

journal homepage: www.sciencedirect.com/journal/organs-on-a-chip

Facile fabrication of microperforated membranes with re-useable SU-8 molds for organs-on-chips

Pim de Haan [a,b], Klaus Mathwig [a,1], Lu Yuan [c], Brandon W. Peterson [c], Elisabeth Verpoorte [a,*]

[a] University of Groningen, Groningen Research Institute of Pharmacy, Pharmaceutical Analysis, P.O. Box 196, 9700 AD Groningen, the Netherlands
[b] TI-COAST, Science Park 904, 1098 XH Amsterdam, the Netherlands
[c] University of Groningen, University Medical Center Groningen, Department of Biomedical Engineering, Antonius Deusinglaan 1, 9713 AV Groningen, the Netherlands

ARTICLE INFO

Keywords:
Poly(dimethylsiloxane)
Microfabrication
SU-8
Porous membrane
Organ-on-a-chip
Gut-on-a-chip

ABSTRACT

Microperforated membranes are essential components of various organ-on-a-chip (OOC) barrier models developed to study transport of molecular compounds and cells across cell layers in *e.g.* the intestine and blood-brain barrier. These OOC membranes have two functions: 1) to support growth of cells on one or both sides, and 2) to act as a filter-like barrier to separate adjacent compartments. Thin, microperforated poly(dimethylsiloxane) (PDMS) membranes can be fabricated by micromolding from silicon molds comprising arrays of micropillars for the formation of micropores. However, these molds are made by deep reactive ion etching (DRIE) and are expensive to fabricate. We describe the micromolding of thin PDMS membranes with easier-to-make, SU-8 epoxy photoresist molds. With a multilayer, SU-8, pillar microarray mold, massively parallel arrays of micropores can be formed in a thin layer of PDMS, resulting in a flexible barrier membrane that can be easily incorporated and sealed between other layers making up the OOC device. The membranes we describe here have a 30-μm thickness, with 12-μm-diameter circular pores arranged at a 100-μm pitch in a square array. We show application of these membranes in gut-on-a-chip devices, and expect that the reported fabrication strategy will also be suitable for other membrane dimensions.

1. Introduction

Organ-on-a-chip (OOC) models emulating elements of the human body at the microscale have become a valuable tool to investigate (patho)physiological processes (Leung et al., 2022; Bhatia and Ingber, 2014). Several of these OOC recapitulate key barrier functions that are present in the body, such as the lung-on-a-chip (Huh et al., 2010), gut-on-a-chip (Mahler et al., 2009; de Haan et al., 2021), and kidney-on-a-chip (Jang et al., 2013). Poly(dimethylsiloxane) (PDMS), a moldable silicone rubber material, has in recent years become popular for the fabrication of OOC devices incorporating barrier functionality. The barriers involved are generally based on porous polymer membranes that act as supports for cell layers, while at the same time separating different biological compartments from one another. In Fig. 1, a schematic diagram of the gut-on-a-chip we have applied in our labs, based on a design by Huh et al. (2013), shows the membrane separating an upper apical chamber from a lower basolateral chamber. To establish the cellular barrier, human or other mammalian cells are cultured on one or both sides of the support membrane, that has often been coated beforehand with a biological matrix to promote cell adhesion (Fig. 1). The material used for membranes may vary from more rigid plastics, such as poly(ethylene terephthalate) (PET), polycarbonate (PC) or polytetrafluoroethylene (PTFE), to the flexible silicone rubber, poly(dimethylsiloxane) (PDMS). All have specific advantages and shortcomings, depending on the application. Commercially available PET, PC, or PTFE membranes have smaller pores, even sub-micrometer-sized, yielding porosities that are more reminiscent of the biological barriers being mimicked. However, they are more difficult to integrate into PDMS-based microfluidic devices. Methods used to fix membranes in microfluidic devices include the application of liquid PDMS pre-polymer to the edges of the plastic membrane, which is then cured at increased temperatures after assembling the device (Chueh et al., 2007; van Midwoud et al., 2010). An alternative approach involves coating the membrane in question with different silanes to promote adhesion of the silane-treated membrane surface to PDMS structures (Aran et al., 2010; Henry et al., 2017).

* Corresponding author.
E-mail address: e.m.j.verpoorte@rug.nl (E. Verpoorte).
[1] Present address: Klaus Mathwig is at imec within OnePlanet Research Center, Bronland 10, 6708 WH Wageningen, the Netherlands.

https://doi.org/10.1016/j.ooc.2023.100026
Received 10 June 2022; Received in revised form 23 December 2022; Accepted 18 January 2023
Available online 20 January 2023

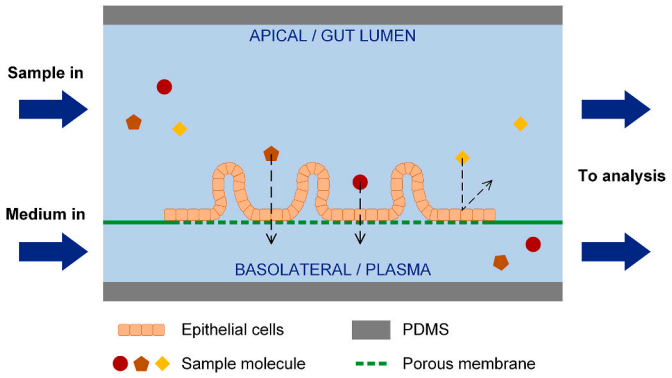

Fig. 1. Schematic of the gut-on-a-chip used in this work, a versatile, representative barrier model that is also used in other OOC (Huh et al., 2013). Two microfluidic channels, termed apical (top, representing the intestinal lumen) and basolateral (bottom, representing the body or plasma compartment) are separated by a thin porous membrane. Epithelial cells are grown on top of this membrane, thus sealing the barrier. Uptake of sample molecules (*e.g.*, drugs, metabolites, nutrients, or toxicants) is facilitated by these cells and may occur via several *trans*- or paracellular pathways, and may occur without or with preceding digestion by artificial digestive juices (de Haan et al., 2019). Irrespective of preceding biochemical processing, the porous membrane is required both to provide stability for the cellular barrier, while at the same time realizing true transfer from apical to basolateral compartments.

For some cases a more flexible membrane is desired, because cells may have different morphologies depending on the stiffness of the substrate (van Oers et al., 2014), or to allow for stretching of cell layers (Huh et al., 2013; Kaarj and Yoon, 2019). To date, PDMS has proven to be the only suitable flexible material available, with the additional advantage that it can be easily bound to glass or PDMS surfaces in microfluidic devices. Membrane flexibility is, however, dictated to a large extent by membrane thickness. For the application at hand, membranes should not exceed a thickness of ~30 μm to achieve the requisite flexibility (Huh et al., 2013). Membranes of this thickness are also more suited to experiments in which cellular layers are meant to act as the natural barrier being mimicked, as the membranes, and thus pores, are thin enough not to act as barriers themselves. Ideally, the membrane used is as thin as possible, and has the highest porosity possible to minimize the inhibition of molecular transport through it. In diffusive transport across the layer, for example, the cells should act as the physiologically relevant barrier that diffusing molecules should overcome, with a negligible contribution to this barrier function by the supporting membrane (Esch et al., 2015). However, large-area porous membranes (tens of mm^2) that are this thin are a challenge to replicate using PDMS (Quirós-Solano et al., 2018), and due to the physical limitations of the molds used and the demolding process, pore diameters cannot be much smaller than 10 μm. For applications involving smaller biological entities like bacteria, these pores may not be small enough. Given that all physiological barriers between the body and the external environment involve epithelial cells, however, these PDMS membranes are appropriate for most OOC applications (intestinal epithelial cells have a cell diameter that is anywhere between 8 and 20 μm). Structures can be patterned into a PDMS layer by micromolding (Duffy et al., 1998), using molds made in photoresist layers on a silicon or glass substrate, or using deep-reactive ion-etched (DRIE) silicon wafers (Huh et al., 2013). DRIE-fabricated silicon wafers are very robust since they are monolithic, but they are expensive to produce, requiring specific plasma-etching instrumentation housed in a cleanroom setting.

Instead of etching silicon wafers, porous membranes may also be fabricated by directly etching a spin-coated PDMS layer at specific places to create holes at high density. This yields excellent results in terms of porosity (up to 65% porosity for 10-μm diameter pores at 11-μm pitch). However, this approach requires long procedures and equipment to specifically coat and etch these materials (Quirós-Solano et al., 2018; Gaio and Quirós-Solano, 2018). Other fabrication methods employ sacrificial structures for making pores. For instance, McClain et al. (2009) described the spin-casting of larger-sized (60 μm) posts that serve as sacrificial structures that need to be removed afterwards. Designed for multilayer microelectronic devices, the pores are somewhat large when considering cell culture on these membranes, as most cells have diameters smaller than 20 μm. Alternatively, Le-The et al. (2018) fabricated sub-micrometer porous membranes by removing sacrificial posts with etchant. While the pores are very small and suited to experiments with organisms the size of bacteria, they require a laborious, multistep procedure. An improved procedure reported by the same group required only one sacrificial layer of photoresist to fabricate microperforated membranes (Zakharova et al., 2020, 2021). Though the membranes produced were very reproducible, neither of these methods allows for re-use of the mold. The methods described in McClain et al. (2009) and Le-The et al. (2018) also require sophisticated cleanroom facilities. We have therefore chosen to pursue a more facile, photoresist-based strategy for the fabrication of porous membranes which does not require removal of sacrificial structures. Moreover, the re-useable molds for these membranes can be produced with standard cleanroom equipment, and the micromolding process to produce the actual membranes may take place outside the cleanroom. The photoresist used is SU-8, an epoxy-based, negative-tone photoresist that is used for numerous applications (del Campo and Greiner, 2007), including the fabrication of molds for microfluidic devices (Duffy et al., 1998). One advantage of SU-8 is its use in high-aspect-ratio applications, with vertical microstructures having height:width ratios on the order of 20 in layers that are 200 μm thick (del Campo and Greiner, 2007). One recent example is an integrated optical device incorporating thin, vertical, reflective SU-8 sheets 30 μm wide and 495 μm high (equivalent to an aspect ratio of 16.5) for the detection of ammonia (Dervisevic et al., 2020). In another example, PDMS membranes were fabricated by spin-coating the PDMS pre-polymer over an array of SU-8 pillars, similar to this work, but without using a stamp on top to seal off the mold, which leads to visual upward protrusions in the pillar areas (Jackman et al., 1999). To make molds, a layer of photoresist is applied to a substrate by spin-coating, with the layer thickness depending on the spinning rate and the viscosity of the photoresist formulation. Typical SU-8 layer thicknesses range from <2 μm to >200 μm per layer spun (Kayaku Advanced Materials, 2020). The photoresist layer is then selectively cured by exposing it to UV light through a photomask, and non-exposed regions are removed during development. The exposed regions remain and form an out-of-plane relief that may be used as a mold for microfluidic devices.

Whereas a molded PDMS chip usually only contains microstructures embedded in one of its surfaces, we employ our molds, containing massively parallel arrays of micro-sized pillars, to introduce through-holes into the layer. The height of the pillars thus determines the thickness of the cast PDMS layers. This work describes the fabrication of 30-μm-thick PDMS membranes with 12-μm-diameter pores separated by a 100-μm-pitch for application in OOC and other devices. We demonstrate the functionality of these membranes by showing their application in a gut-on-a-chip, in which a layer of human intestinal cells was cultured on top of this membrane. The overall methodology in this work may also be used in other organ-on-a-chip applications, as well as other microtechnological applications.

2. Materials and methods

The fabrication procedure for porous membranes is described below. The fabrication of the SU-8 molds used is based in part on the SU-8 manufacturer's guidelines (Microchem. SU-8 Processing, 2020). For the molding of thin PDMS membranes, a PDMS structure transferring strategy first described by Zhang et al. (2010) and modified by Kung et al. (2015) has been applied. This approach first sees PDMS in its prepolymer liquid form cast over the pillar arrays to completely cover all

the pillars. This viscous layer is then depressed using a very flat slab of PDMS treated with fluorinated trichlorosilane, until the tops of the pillars are in contact with the slab. Once cured, the cast layer of PDMS can easily be demolded by peeling the PDMS slab from the mold, as this thin layer adheres more to the PDMS slab than to the mold. The PDMS slab thus serves as a handle to transfer the thin membrane from the mold to the microfluidic device, where the membrane is aligned with microfluidic channels and is subsequently separated from the slab. Membrane parameters (30 μm thickness, 10 × 1 mm membrane suspension area) were based on gut-on-a-chip devices as described in the literature (Huh et al., 2013; Kim et al., 2012). SU-8 is available in different formulations for specific thickness ranges; the two formulations used in this protocol have ranges of 2.0–4.0 and 10–30 μm (SU-8 2002 and SU-8 10, respectively) (Microchem. SU-8 Processing, 2020).

2.1. Materials and apparatus

SU-8 2002 and SU-8 10 (Kayaku, Westborough, MA, USA) were spin-coated onto glass wafers (10 cm diameter Borofloat 33, 700 μm thickness, 10 cm diameter, Handelsagentur Helmut Teller, Jena, Germany) with a spin-coater housed in a standard cleanroom. A 0.2-μm-resolution photomask (chromium on soda-lime glass, darkfield, Delta Mask, Enschede, the Netherlands) was used to pattern structures by illumination with a collimated UV light source at 365 nm (OAI model 30/5, Milpitas, CA, USA). All baking steps were performed on a programmable hotplate under aspiration of fumes. Non-exposed SU-8 was removed by incubating the mold with SU-8 Developer (mr-Dev 600, 1-methoxy-2-propanol acetate, Micro Resist Technology, Berlin, Germany) under gentle shaking. PDMS (Sylgard 184, Dow Corning, Midland, MI, USA) was mixed manually at a 15:1 ratio (elastomer base/curing agent) and gas bubbles were removed using a vacuum desiccator. To facilitate demolding, molds were coated in a vapor of 1H,1H,2H,2H-perfluorooctyl trichlorosilane (PFOTCS, Sigma-Aldrich, Zwijndrecht, the Netherlands) in another (dedicated) vacuum desiccator. Bonding of PDMS to other surfaces (PDMS or glass) was done using an oxygen plasma cleaner (PDC-0002, Harrick Plasma, Ithaca, NY, USA).

2.2. Fabrication of molds

Molds for the porous membranes were fabricated in a standard cleanroom. A chromium-on-glass photomask was designed using CleWin (Wieweb Software, Hengelo, the Netherlands) to contain a square array of circular holes (12 μm diameter, 100 μm pitch, 25 × 25 mm footprint). Each array contained 250 × 250 holes, for a total of 62,500 holes. The molds were fabricated according to the following procedure (letters in parentheses refer to Fig. 2). Before each UV exposure, the actual intensity of the light source (λ = 365 nm) was measured (mW/cm^2) to calculate the exact exposure time to tenths of seconds (OAI 306 UV power meter).

1. A glass wafer is cleaned with acetone, isopropanol, and water, then spun dry.
2. The wafer is thoroughly dehydrated at 150 °C for at least 30 min.
3. A 4-μm-thick adhesion promoting sublayer of SU-8 2002 is spin-coated onto the wafer at 500 rpm for 35 s, and soft-baked at 95 °C for 2 min on a level hotplate.
4. The entire SU-8 sublayer is exposed to 145 mJ/cm^2 UV light and then heated to 95 °C for 2.5 min as post-exposure bake to

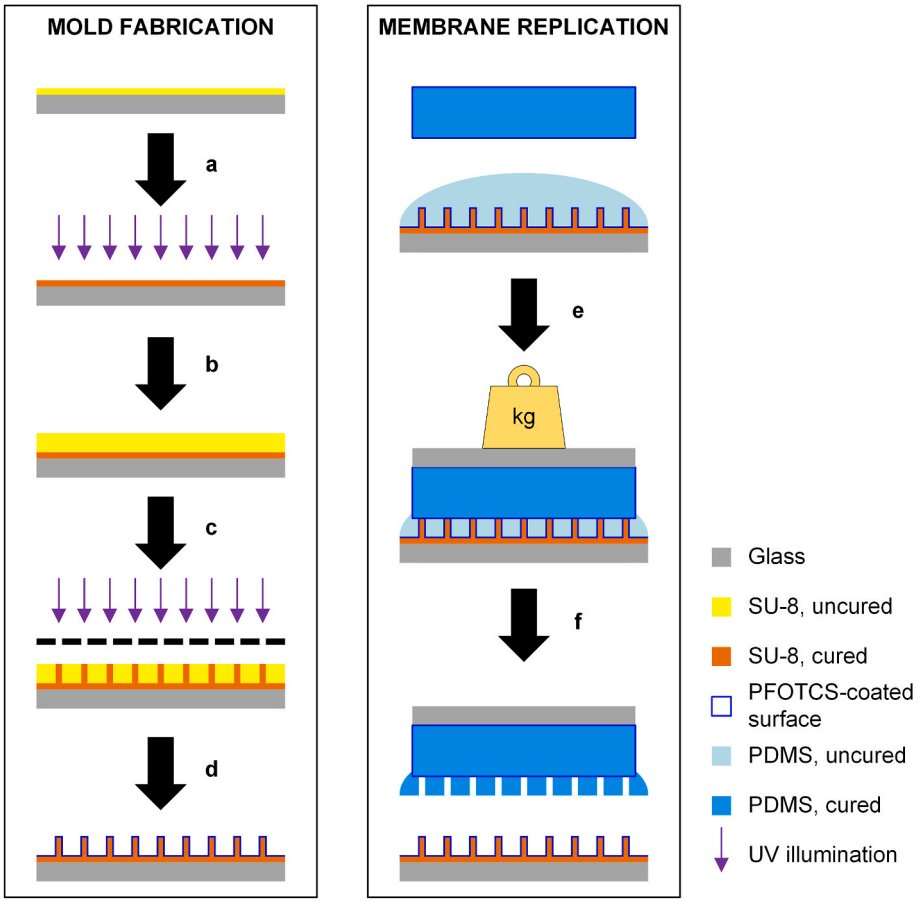

Fig. 2. Schematic of the fabrication process of two-layer SU-8 molds (a–d) and porous PDMS membranes (e–f). The fabrication steps are described in detail in the main text.

optimize crosslinking of the SU-8 in exposed regions, followed by a subsequent hard-bake at 150 °C for 20 min (Step a) on a level hotplate. The wafer is allowed to cool down passively to room temperature on a tissue on the wet bench.

5. The SU-8 layer is then exposed to oxygen plasma (29 W) for 30 s to activate the surface and improve adhesion of the second SU-8 layer.
6. A 30-μm-thick layer of SU-8 10 is spin-coated on top of the first layer (500 rpm for 5 s, then 1000 rpm for 30 s), and soft-baked on a programmable hotplate with the following temperature program: 30 min at room temperature; temperature ramped to 65 °C in 45 min; temperature maintained at 65 °C for 3 min before ramping up to 95 °C in 30 min; temperature kept constant at 95 °C for 7 min before finally cooling down the wafer passively on a cooling hotplate (Step b).
7. The photomask is brought into conformal contact with the SU-8 layer, which is then exposed to UV light (300 mJ/cm^2) and post-exposure baked using the following temperature program: temperature is ramped from room temperature to 65 °C in 45 min, kept constant at 65 °C for 1 min; ramped to 95 °C in 30 min; kept constant for 3 min and allowed to cool down passively on the hotplate (Step c).
8. Uncured SU-8 is dissolved in SU-8 Developer for 5 min in a crystallizing dish under gentle agitation; the solvent is refreshed, and the wafer is incubated for another 2 min (Step d).
9. The mold is washed thoroughly with isopropanol and hard-baked at 150 °C for 20 min.
10. A silane coating is applied to the mold by incubating it *in vacuo* with 10 μL of PFOTCS for at least 4 h. The 10 μL of PFOTCS is pipetted onto a watch glass placed on the bottom of the desiccator kept inside a fume hood. The vacuum is applied by a continuously running membrane pump to enhance evaporation of the silane. The chlorine atoms act as leaving groups upon covalently binding of the silane to the solid glass or SU-8 surface.

2.3. Fabrication of porous membranes

The process for making the thin, porous PDMS membranes is depicted in the righthand column of Fig. 2. A step-for-step procedure is given below (letters in parentheses refer to steps shown in Fig. 2).

2.3.1. PDMS handle for structure transfer

PDMS elastomer and curing agent are mixed at a 10:1 ratio and degassed *in vacuo* for 30 min.

11. A 5-mm-thick layer of PDMS is cast onto a bare, silanized glass wafer on a sheet of aluminum foil with the edges folded upwards to contain the PDMS prepolymer (silanization step is the same as in Step 10, Section 2.2) and cured on a 70 °C hotplate for 2 h.
12. The cured PDMS is then cut into square slabs of 2 × 2 cm.
13. The PDMS slabs are exposed to oxygen plasma (29 W) for 30 s, and incubated *in vacuo* with 10 μL of PFOTCS for 1 h.
14. For the membranes, PDMS elastomer and curing agent are mixed at a 15:1 ratio for higher flexibility (Huh et al., 2013), and degassed *in vacuo* for 30 min (Note that this ratio is different from the 10:1 ratio usually employed for making microfluidic devices (Duffy et al., 1998) and the PDMS slab above.)

2.3.2. Replication of membrane

15. A small amount of this PDMS mixture is poured onto the mold to cover all the pillars completely over an area of about 1 cm in diameter. The mold is then placed on a level hotplate.
16. One silanized PDMS slab (made in Step 12 to 14) is carefully placed on top of the cast PDMS, while applying gentle pressure to force the excessive liquid PDMS out, and to make the PDMS slab rest on top of the pillar array (Step e). Pressure is applied by thumb, in order to detect if the slab is in contact with the top of the pillars. If the applied pressure is not enough, and a thin film of liquid PDMS remains between the top of the pillars and the surface of the PDMS slab, it will be possible to move the slab laterally. In contrast, if contact between the pillars and the PDMS slab is established, the slab will not be able to move laterally.
17. A glass microscope slide is placed on top of the slab, and a weight is added to keep the slab in position (340 g, ~8.3 kPa) (Step e).
18. The assembly is kept on the hotplate at room temperature overnight, for curing at 60 °C for 1 h the next day on the same hotplate. In this way, any liquid PDMS between the stamp and the top of the mold slowly escapes until the stamp fully touches the top of the mold. The assembly does not have to be transferred from another location, eliminating the risk of interfering with the curing process.
19. After passive cooling to room temperature, the weight and microscope slide are removed. A small (~10 μL) droplet of absolute ethanol is applied to the PDMS-mold interface to facilitate demolding by carefully lifting the slab, starting at a corner. By doing so, the membrane remains stuck to the surface of the slab (handle), making it easy to handle and store (Step f). Excess PDMS around the edges of the PDMS slab could be removed by tearing it off manually.

2.4. Integration of membrane into a microfluidic OOC device

In this section, we consider the integration of the porous membrane into a microfluidic OOC device like that shown in Fig. 3. This device is a typical example of an OOC barrier model, and has been used as a gut-on-a-chip for absorption and other studies (Huh et al., 2013; Yuan et al., 2020). The membrane separates an upper chamber, having a channel layout as shown in this figure, from a lower chamber having the same layout, but flipped 180°. The middle segment of the top and bottom channels overlaps; it is in this region of the device that cells are cultured to establish a biological barrier function. All inlets and outlets are found on the top surface, and the two solutions flow past the membrane as indicated by the red and blue arrows. This device is modelled after a design presented by Huh et al., 2010, 2013.

20. For integration into a three-layer microfluidic device (Fig. 3), one slab of PDMS containing a channel structure and the PDMS membrane (still on the PFOTCS-coated handle) are treated with oxygen plasma (29 W, 30 s). The channel-containing slab is treated with the channel side up for exposure to oxygen plasma.
21. The treated surfaces of the two pieces are brought into conformal contact with the PDMS handle with membrane on top, and the assembled pieces are heated to 60 °C for 1 h. This thermal treatment improves bonding strength and causes the surface of the plasma-exposed membrane and channel walls to re-assume their original hydrophobic state. Otherwise, there would be a risk of the membrane collapsing and bonding to the channel walls.
22. A microdroplet (0.5 μL) of absolute ethanol is applied to the membrane-handle interface to facilitate removal of the PFOTCS-coated slab, leaving the porous membrane behind to cover the microfluidic channel.
23. The membrane-channel assembly and the other slab containing a channel structure are treated with oxygen plasma (29 W, 30 s) as described above, aligned (with the membrane-channel assembly on top of the second slab with channel), and bonded together. The device is heated to 60 °C for 1 h to increase the bonding strength.

After being used several times, the mold for membranes was cleaned with isopropanol and oxygen plasma (29 W, 30 s) and resilanized with PFOTCS (Section 2.2, Step 10). Torn-off pieces of membranes could be removed by covering them with an excess of PDMS prepolymer (15:1, as

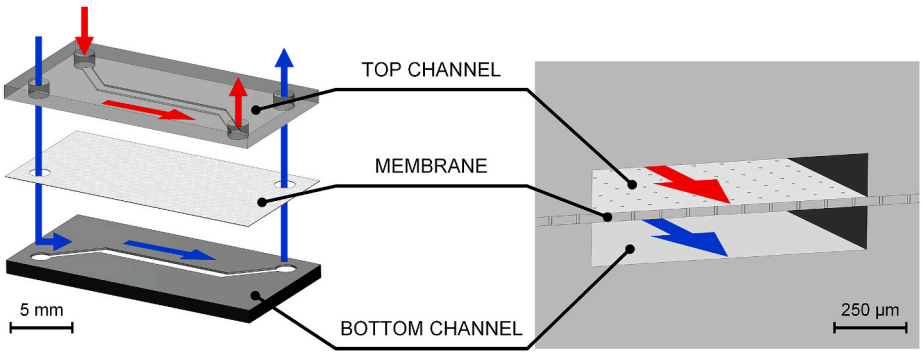

Fig. 3. Exploded view and cross-sectional 3D rendering of the three-layer gut-on-a-chip assembly, showing the bottom channel, porous membrane, and the top channel layer. All fluidic access holes are located at the top. Both channels are 1000 µm wide and 150 µm deep, and the straight channel segment in the center (which contains the suspended membrane) is 10 mm long. Access holes are 1.5 mm in diameter. For optimal inspection by inverted light microscope, the PDMS slab containing the bottom channel is only 1–2 mm thick. The slab with the top channel is around 4 mm thick in order to fix the tubing directly inside the punched access holes.

above), curing this at 70 °C for 2 h, and peeling off the cured PDMS with the pieces embedded in it. Methods for cell culturing and the preparation of gut-on-a-chip devices are reported in detail elsewhere (Huh et al., 2013; Kim et al., 2015). In short, human intestinal epithelium cells (Caco-2 BBE, from ATCC, Manassas, VA, USA) were cultured in Dulbecco's Modified Eagle Medium (DMEM) supplemented with 25 mM glucose, GlutaMAX, 100 U/mL penicillin, 100 µg/mL streptomycin, 25 mM HEPES, and 10% v/v fetal bovine serum (all from ThermoFisher, Waltham, MA, USA). Caco-2 cells of passages 52–54 were seeded into the OOC described here at a density of 150,000 cells/cm^2. At this density, the cell layer is almost confluent upon adhesion of the cells to the porous membrane. Flows of cell medium were started 2 h after seeding at 30 µL/h in both channels of the OOC.

3. Results and discussion

Photographs of the fabricated molds and membranes are shown in Fig. 4. The arrays of pillars used as molds (Fig. 4a and b) were very regular, and no defects were visible upon fabrication of these molds. The shorter (1 h; Step 11) treatment of the PDMS handles with PFOTCS, as opposed to the longer (4 h) treatment of the molds, led to a better detachment of the membrane from the mold. Approximately equal silanization times led to more difficult detachment of the membrane from the mold and tearing of the membrane. Once detached from the mold, the membrane remained attached to the (transparent) PDMS handle for easier handling and aligning before bonding to the channel structures.

It was found to be essential to include a 1-h heating step at 60 °C (Step 22) before removing the PDMS handle, as this heating step is thought to accelerate the hydrophobic recovery of the oxygen plasma-treated PDMS (Eddington et al., 2006; Senzai and Fujikawa, 2019). The mechanism for hydrophobic recovery is still debated, but an often described explanation is the possible migration of non-polymerized fragments from within the polymer matrix to its surface (Eddington

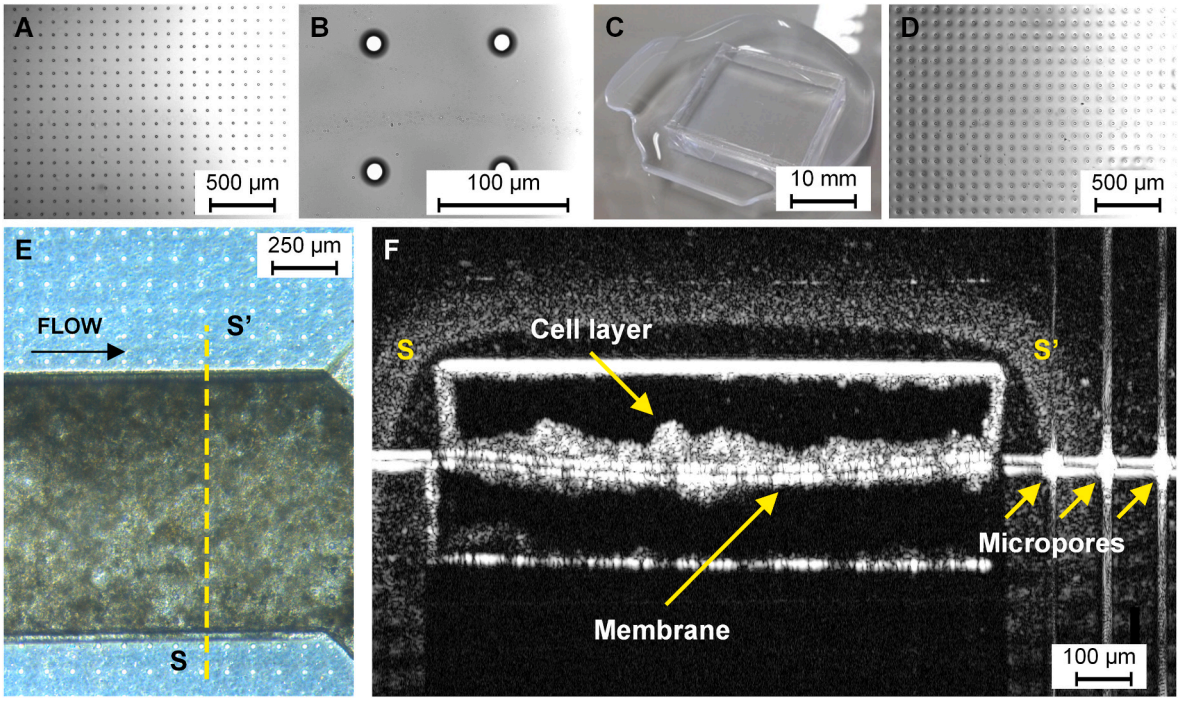

Fig. 4. (**a**) and (**b**) Optical micrographs of the mold with pillar array (12 µm diameter, 100 µm pitch, 30 µm height,). (**c**) Inverted block of PDMS serving as handle (2×2 cm), with the membrane adhered onto the top surface. (**d**) Micrograph of the membrane before assembling. (**e**) Gut-on-a-chip device (top view), with Caco-2 intestinal epithelial cells (appearing brown) grown on top of the porous PDMS membrane, four days after cell seeding. Viewed from above, membrane pores confined between two PDMS surfaces are visible as a regular array of white circles. (**f**) The internal structures in the channel become visible using optical coherence tomography (Yuan et al., 2020). In this cross-section (see line S–S′ in panel E), the membrane surface is visible as two horizontal white lines. Cells are visible as cloudy structures on top of the membrane. Three micropores on the right fall directly in the imaging plane of this cross-sectional view, causing optical artefacts at the right (vertical white lines). (For interpretation of the references to colour in this figure legend, the reader is referred to the Web version of this article.)

et al., 2006; Senzai and Fujikawa, 2019). Without this heating step, the PDMS surface remained slightly activated and the membrane could accidentally bond irreversibly to the channel walls. A minimal volume of ethanol (0.5 μL) was used to facilitate the removal of the PDMS-handle slab from the membrane. Ethanol helps to demold by wicking into the space between the two PDMS surfaces, but larger volumes were found to fill the underlying channel structure through the pores. The ethanol then pulled the membrane down to the bottom channel surface while evaporating from the channel, causing the membrane to stick there and deform. Using a small enough volume of ethanol eliminates this problem. It should also be noted that reuse of the silanized PDMS-handle slabs for another round of fabrication proved not to be successful.

Micrographs of the PDMS membrane show good molding results, and the pores were visible after assembling the three-layer gut-on-a-chip device (Fig. 4d and e). Cells readily attached to the membrane surface that had been coated with extracellular matrix (ECM, containing 50 μg/mL collagen type I and 300 μg/mL Matrigel in serum-free cell medium) beforehand (Fig. 4e) (Kim et al., 2015; Kim and Ingber, 2013; Kasendra et al., 2018). The cell layer became visible in a cross-sectional view of the gut-on-a-chip with spectral-domain optical coherence tomography (OCT) (Fig. 4f), showing three-dimensional structures arising from the membrane surface (visible in white) (Yuan et al., 2020). The presence of cells after four days of culturing (Fig. 4e and f) indicates that cells thrive when grown on top of this ECM-coated PDMS membrane; adherent cells such as the Caco-2 cells used in this study normally detach from the surface upon cell death. Supplementary Fig. 1 shows bright-field micrographs of this gut-on-a-chip over time, as well as fluorescent staining of live epithelial cells with calcein AM on the sixth day after seeding. Calcein AM is converted to a green fluorescent molecule intracellularly, exclusively by living cells. The presence of fluorescence throughout the microchannel therefore proves the viability of the cells cultured therein.

The flexibility of the membrane provides a more *in vivo*-like substrate for intestinal cells by allowing for lateral stretching of these cell layers. Forces across the membrane area can be applied either pneumatically (Huh et al., 2010) or electrostatically, as part of a dielectric elastomer actuator (Poulin et al., 2018). The fabrication method described in this paper can be used for the fabrication of flexible perforated membranes, with holes patterned through the entire membrane; as opposed to regular PDMS micromolding approaches, where structures are patterned into (but not all the way through) a layer of PDMS. Methods to create open structures completely through a thin layer of PDMS have been described before (Zhang et al., 2010; Kung et al., 2015), but these were found to be unsuitable for the easy reproduction of massive arrays of holes through the layer. Zhang et al. first described a method to fabricate thin PDMS layers with channel structures patterned as through-holes (Zhang et al., 2010). PFOTCS-treated blocks were used to press the liquid PDMS down onto a mold while curing, at a pressure of 200–300 kPa. Kung et al. observed that patterned PDMS layers produced with this method often have protruding edges due to the elasticity of the stamp that is used when pressing the PDMS down (Kung et al., 2015). They therefore embedded a rigid polystyrene layer inside the PDMS handle or stamp in order to increase its Young's modulus. The block was placed onto the mold with liquid PDMS during curing at a pressure of ~28 kPa. We found that both these pressure levels were too high for use in massive micropillar arrays, as they led to vast damage to the micropillars of the mold. In fact, the amount of pressure we used (~8.3 kPa) was found to be essential for good membranes. Too little pressure caused the PDMS slab to lose contact with the top of the pillars, leading to the pores being closed on one side; too much pressure could lead to a reduced flatness of the membrane and could damage the pillars on the mold (which have an aspect ratio of 2.5:1). The pressure we used is less than half of what Kung et al. (2015) used, and this led to the best result using these pillar arrays. In the same paper, a sacrificial layer of polystyrene was used inside the stamp, which could be dissolved to remove the stamp (handle). In our fabrication strategy, inclusion of a sacrificial plastic layer was not necessary to obtain good membranes. The edge protruding effect that is prevented by this method reportedly occurs at multiple hundreds of micrometers from the edge of the mold structures, and in this particular situation, the micropillars are placed at a 100-μm pitch. This is well within this distance, preventing visible edge protrusions. Another improvement we report is the inclusion of a 30-s oxygen plasma treatment step to activate the surface of the PDMS blocks, before treating them with PFOTCS. As the contact area between the micropillars of the mold and the newly formed porous PDMS membrane is vast, an improved surface coating with the silane was necessary to be able to demold the membrane without tearing. We expect that the same procedure can be used to mold larger arrays of microstructures, provided that the same pressure is used and the pressure is evenly distributed over the mold. A higher density of pillars (*i.e.*, a smaller pitch between the pillars of 25 or 40 μm) was tried in the same fashion, however, the resulting PDMS membranes were found impossible to de-mold without extensive tearing, even when using a slightly smaller pillar diameter (10 μm). As alluded to in the introduction, the porosity should ideally be as high as possible to avoid any hindrance of molecular transport through the cell layer as result of the membrane. The presence of three-dimensional villus-like structures mitigates this effect to some extent, by creating an intercellular space between the basolateral side of the cells and the top of the membrane (Fig. 1).

The yield of the mold fabrication is 100%, as these processes were performed in a controlled environment in a well-maintained cleanroom, where standard procedures for photolithographic patterning had already been established and optimized. The yield of membrane fabrication is estimated somewhere between 75 and 90%, as some membranes tore upon de-molding; however, this is not necessarily destructive as the remaining membrane area is still generally large enough to be used in an OOC. The molds could be reused three to four times after resilanization, for a maximum of five times of silanization (*i.e.* a total of 20 fabricated membranes per glass wafer containing four molds).

4. Conclusions

The fabrication procedure we report enables the fabrication and efficient handling of thin PDMS membranes, into which massive arrays of through holes are patterned. It is the first simple micromolding strategy that has been reported to yield micropore through holes based on SU-8 micromolding, eliminating the need for more expensive deep reactive ion-etched silicon wafers. The novelty of this work lies in the combination of these two aspects: the use of massive arrays of SU-8 micropillars as a re-useable mold, and their molding as through holes as opposed to the usual dead-end cavities. The resulting membranes are suitable for application in OOC devices, such as the gut-on-a-chip shown. This fabrication procedure is facile and relatively fast in the production of microperforated membranes, whereas commercial membranes tend to be either made out of rigid plastics, or have a higher cost when fabricated by track-etching a PDMS film. The flexible membranes described here have a thickness of 30 μm, with 12-μm-diameter pores at a 100 μm pitch. We expect that this fabrication procedure is suitable for other dimensions as well. We hypothesize that the limiting factor is the demolding step: arrays of high-aspect-ratio (11:1) SU-8 pillars have been described (Amato et al., 2012), and the molding of PDMS slabs with massive arrays of micropillars in SU-8 and other photoresists has also been described (Slentz et al., 2001). The difficulty lies in the combination of 1) the sub-30-μm thickness of membranes, which makes it prone to tearing; 2) the patterning of through holes rather than imprints in just one side of a thicker, self-supporting slab of PDMS; and 3) the relatively large contact area between mold and PDMS, which increases adhesion of the membrane structure to the mold. The molds used in this work are fairly robust: the flat sublayer of SU-8 enhances the anchoring of pillars to the wafer, enabling re-use of the mold for 3–4 times before it needs to be resilanized. Improper coating with PFOTCS was manifested by the inability to demold the thin membranes rather than damage to the mold

(*e.g.* pillar breakage), which was stable enough to be reused several times. For future research, other membrane dimensions may be investigated, with the assumption that the relative contact area (*i.e.* the total contact area of a membrane section to the mold divided by the product of its length and width) is likely to be the essential parameter for successful demolding. If this assumption holds, the fabrication of higher-porosity membranes should be possible if the membrane thickness decreases somewhat.

Author contributions

Conceptualization, P.d.H., K.M., and E.V.; methodology, P.d.H., K.M., and E.V.; investigation, P.d.H.; resources, L.Y. and B.W.P.; writing—original draft preparation, P.d.H., K.M., and E.V.; writing—review and editing, all authors; visualization, P.d.H. and L.Y.; supervision, E.V.; project administration, E.V.; funding acquisition, E.V. All authors have read and agreed to the published version of the manuscript.

Funding

This research was funded by the Dutch Research Council (NWO) in the framework of Technology Area PTA-COAST3, grant number 053.21.116 (GUTTEST), of the Fund New Chemical Innovations.

Declaration of competing interest

The authors declare that they have no known competing financial interests or personal relationships that could have appeared to influence the work reported in this paper.

Data availability

Data will be made available on request.

Appendix A. Supplementary data

Supplementary data to this article can be found online at https://doi.org/10.1016/j.ooc.2023.100026.

References

Amato, L., Keller, S.S., Heiskanen, A., Dimaki, M., Emnéus, J., Boisen, A., et al., 2012. Fabrication of high-aspect ratio SU-8 micropillar arrays. Microelectron. Eng. 98, 483–487. https://doi.org/10.1016/j.mee.2012.07.092.

Aran, K., Sasso, L.A., Kamdar, N., Zahn, J.D., 2010. Irreversible, direct bonding of nanoporous polymer membranes to PDMS or glass microdevices. Lab Chip 10, 548–552. https://doi.org/10.1039/b924816a.

Bhatia, S.N., Ingber, D.E., 2014. Microfluidic organs-on-chips. Nat. Biotechnol. 32, 760–772. https://doi.org/10.1038/nbt.2989.

Chueh, B.H., Huh, D., Kyrtsos, C.R., Houssin, T., Futai, N., Takayama, S., 2007. Leakage-free bonding of porous membranes into layered microfluidic array systems. Anal. Chem. 79, 3504–3508. https://doi.org/10.1021/ac062118p.

del Campo, A., Greiner, C., 2007. SU-8: a photoresist for high-aspect-ratio and 3D submicron lithography. J. Micromech. Microeng. 17, R81–R95. https://doi.org/10.1088/0960-1317/17/6/R01.

Dervisevic, E., Voelcker, N.H., Risbridger, G., Tuck, K.L., Cadarso, V.J., 2020. High-aspect-ratio SU-8-based optofluidic device for ammonia detection in cell culture media. ACS Sens. 5, 2523–2529. https://doi.org/10.1021/acssensors.0c00821.

Duffy, D.C., McDonald, J.C., Schueller, O.J.A., Whitesides, G.M., 1998. Rapid prototyping of microfluidic systems in poly(dimethylsiloxane). Anal. Chem. 70, 4974–4984. https://doi.org/10.1021/ac980656z.

Eddington, D.T., Puccinelli, J.P., Beebe, D.J., 2006. Thermal aging and reduced hydrophobic recovery of polydimethylsiloxane. Sens. Actuators B Chem. 114, 170–172. https://doi.org/10.1016/j.snb.2005.04.037.

Esch, E.W., Bahinski, A., Huh, D., 2015. Organs-on-chips at the frontiers of drug discovery. Nat. Rev. Drug Discov. 14, 248–260. https://doi.org/10.1038/nrd4539.

de Haan, P., Ianovska, M.A., Mathwig, K., van Lieshout, G.A.A., Triantis, V., Bouwmeester, H., et al., 2019. Digestion-on-a-chip: a continuous-flow modular microsystem recreating enzymatic digestion in the gastrointestinal tract. Lab Chip 19, 1599–1609. https://doi.org/10.1039/c8lc01080c.

de Haan, P., Santbergen, M.J.C., van der Zande, M., Bouwmeester, H., Nielen, M.W.F., Verpoorte, E., 2021. A versatile, compartmentalised gut-on-a-chip system for pharmacological and toxicological analyses. Sci. Rep. 11 https://doi.org/10.1038/s41598-021-84187-9. Art. Nr. 4920.

Gaio, N., Quiros Solano, W., 2018. Versatile 3D stretchable micro-environment for organ-on-chip devices fabricated with standard silicon technology. Patent WO2018021906. WO2018021906.

Henry, O.Y.F., Villenave, R., Cronce, M.J., Leineweber, W.D., Benz, M.A., Ingber, D.E., 2017. Organs-on-chips with integrated electrodes for trans-epithelial electrical resistance (TEER) measurements of human epithelial barrier function. Lab Chip 17, 2264–2271. https://doi.org/10.1039/C7LC00155J.

Huh, D., Matthews, B.D., Mammoto, A., Montoya-Zavala, M., Hsin, H.Y., Ingber, D.E., 2010. Reconstituting organ-level lung functions on a chip. Science 328, 1662–1668. https://doi.org/10.1126/science.1188302.

Huh, D., Kim, H.J., Fraser, J.P., Shea, D.E., Khan, M., Bahinski, A., et al., 2013. Microfabrication of human organs-on-chips. Nat. Protoc. 8, 2135–2157. https://doi.org/10.1038/nprot.2013.137.

Jackman, R.J., Duffy, D.C., Cherniavskaya, O., Whitesides, G.M., 1999. Using elastomeric membranes as dry resists and for dry lift-off. Langmuir 15, 2973–2984. https://doi.org/10.1021/la981591y.

Jang, K.-J., Mehr, A.P., Hamilton, G.A., McPartlin, L.A., Chung, S., Suh, K.-Y., et al., 2013. Human kidney proximal tubule-on-a-chip for drug transport and nephrotoxicity assessment. Integr. Biol. 5, 1119–1129. https://doi.org/10.1039/c3ib40049b.

Kaarj, K., Yoon, J.-Y., 2019. Methods of delivering mechanical stimuli to organ-on-a-chip. Micromachines 10. https://doi.org/10.3390/mi10100700. Art. Nr. 700.

Kasendra, M., Tovaglieri, A., Sontheimer-Phelps, A., Jalili-Firoozinezhad, S., Bein, A., Chalkiadaki, A., et al., 2018. Development of a primary human Small Intestine-on-a-Chip using biopsy-derived organoids. Sci. Rep. 8 https://doi.org/10.1038/s41598-018-21201-7. Art. Nr. 2871.

Kayaku Advanced Materials. SU-8 Photoresist. n.d. https://kayakuam.com/products/su-8-photoresists/. (Accessed 3 July 2020).

Kim, H.J., Ingber, D.E., 2013. Gut-on-a-Chip microenvironment induces human intestinal cells to undergo villus differentiation. Integr. Biol. 5, 1130–1140. https://doi.org/10.1039/c3ib40126j.

Kim, H.J., Huh, D., Hamilton, G., Ingber, D.E., 2012. Human gut-on-a-chip inhabited by microbial flora that experiences intestinal peristalsis-like motions and flow. Lab Chip 12, 2165–2174. https://doi.org/10.1039/c2lc40074j.

Kim, H.J., Li, H., Collins, J.J., Ingber, D.E., 2015. Contributions of microbiome and mechanical deformation to intestinal bacterial overgrowth and inflammation in a human gut-on-a-chip. Proc. Natl. Acad. Sci. USA 113, E7–E15. https://doi.org/10.1073/pnas.1522193112.

Kung, Y.-C., Huang, K.-W., Fan, Y.-J., Chiou, P.-Y., 2015. Fabrication of 3D high aspect ratio PDMS microfluidic networks with a hybrid stamp. Lab Chip 15, 1861–1868. https://doi.org/10.1039/C4LC01211A.

Le-The, H., Tibbe, M., Loessberg-Zahl, J., Palma do Carmo, M., van der Helm, M., Bomer, J., et al., 2018. Large-scale fabrication of free-standing and sub-μm PDMS through-hole membranes. Nanoscale 10, 7711–7718. https://doi.org/10.1039/C7NR09658E.

Leung, C.M., de Haan, P., Ronaldson-Bouchard, K., Kim, G.-A., Ko, J., Rho, H.S., et al., 2022. A guide to the organ-on-a-chip. Nat. Rev. Methods Primers 2. https://doi.org/10.1038/s43586-022-00118-6. Art. Nr. 33.

Mahler, G.J., Esch, M.B., Glahn, R.P., Shuler, M.L., 2009. Characterization of a gastrointestinal tract microscale cell culture analog used to predict drug toxicity. Biotechnol. Bioeng. 104, 193–205. https://doi.org/10.1002/bit.22366.

McClain, M.A., LaPlaca, M.C., Allen, M.G., 2009. Spun-cast micromolding for etchless micropatterning of electrically functional PDMS structures. J. Micromech. Microeng. 19 https://doi.org/10.1088/0960-1317/19/10/107002. Art. Nr. 107002.

Microchem, 2020. SU-8 Processing Guidelines. Microchem. Newton, MA, USA.

van Midwoud, P.M., Groothuis, G.M.M., Merema, M.T., Verpoorte, E., 2010. Microfluidic biochip for the perifusion of precision-cut rat liver slices for metabolism and toxicology studies. Biotechnol. Bioeng. 105, 184–194. https://doi.org/10.1002/bit.22516.

van Oers, R.F.M., Rens, E.G., LaValley, D.J., Reinhart-King, C.A., Merks, R.M.H., 2014. Mechanical cell-matrix feedback explains pairwise and collective endothelial cell behavior in vitro. PLoS Comput. Biol. 10, 1–14. https://doi.org/10.1371/journal.pcbi.1003774.

Poulin, A., Imboden, M., Sorba, F., Grazioli, S., Martin-Olmos, C., Rosset, S., et al., 2018. An ultra-fast mechanically active cell culture substrate. Sci. Rep. 8 https://doi.org/10.1038/s41598-018-27915-y. Art. Nr. 9895.

Quirós-Solano, W.F., Gaio, N., Stassen, O.M.J.A., Arik, Y.B., Silvestri, C., van Engeland, N.C.A., et al., 2018. Microfabricated tuneable and transferable porous PDMS membranes for Organs-on-Chips. Sci. Rep. 8 https://doi.org/10.1038/s41598-018-31912-6. Art. Nr. 13524.

Senzai, T., Fujikawa, S., 2019. Fast hydrophobicity recovery of the surface-hydrophilic poly(dimethylsiloxane) films caused by rechemisorption of dimethylsiloxane derivatives. Langmuir 35, 9747–9752. https://doi.org/10.1021/acs.langmuir.9b01448.

Slentz, B.E., Penner, N.A., Lugowska, E., Regnier, F., 2001. Nanoliter capillary electrochromatography columns based on collocated monolithic support structures molded in poly(dimethyl siloxane). Electrophoresis 22, 3736–3743. https://doi.org/10.1002/1522-2683(200109)22:17<3736::AID-ELPS3736>3.0.CO;2-Y.

Yuan, L., de Haan, P., Peterson, B.W., de Jong, E.D., Verpoorte, E., van der Mei, H.C., et al., 2020. Visualization of bacterial colonization and cellular layers in a gut-on-a-chip system using optical coherence tomography. Microsc. Microanal. 26, 1211–1219. https://doi.org/10.1017/S143192762002454X.

Zakharova, M., Palma do Carmo, M.A., van der Helm, M.W., Le-The, H., de Graaf, M.N.S., Orlova, V., et al., 2020. Multiplexed blood–brain barrier organ-on-chip. Lab Chip 20, 3132–3143. https://doi.org/10.1039/D0LC00399A.

Zakharova, M., Tibbe, M.P., Koch, L.S., Le-The, H., Leferink, A.M., van den Berg, A., et al., 2021. Transwell-integrated 2 μm thick transparent polydimethylsiloxane membranes with controlled pore sizes and distribution to model the blood-brain barrier. Adv. Mater. Technol. 6 https://doi.org/10.1002/admt.202100138. Art. Nr. 2100138.

Zhang, M., Wu, J., Wang, L., Xiao, K., Wen, W., 2010. A simple method for fabricating multi-layer PDMS structures for 3D microfluidic chips. Lab Chip 10, 1199. https://doi.org/10.1039/b923101c.